Diagrammatic analysis of QCD gauge transformations and gauge cancellations

Y. J. Feng* and C. S. Lam†
Department of Physics, McGill University, 3600 University Street, Montreal, Quebec, Canada H3A 2T8
(Received 13 March 1995)

Diagrammatic techniques are invented to implement QCD gauge transformations. These techniques can be used to discover how gauge-dependent terms are canceled among diagrams to yield gauge-invariant results in the sum. In this way a multiloop pinching technique can be developed to change ordinary vertices into background-gauge vertices. The techniques can also be used to design new gauges to simplify calculations by reducing the number of gauge-dependent terms present in the intermediate steps. Two examples are discussed to illustrate this aspect of the applications.

PACS number(s): 11.15.Bt

I. INTRODUCTION

A typical computation in the standard model generates many gauge-dependent terms that get canceled at the end. The labor of calculation can be thus considerably reduced if suitable gauges are chosen to minimize the presence of these terms. As far as propagators go it is usually simplest to use the Feynman gauge. As to vertices and external gluon wave functions, more unconventional gauges can often lead to greater simplifications.

The spinor helicity technique [1] is a case in point. External gluon wave functions are chosen in light cone gauges defined by lightlike reference momenta k, which may be different for different gluons. A judicious choice of k's can reduce the number of terms present, and sometimes even renders whole diagrams zero. This technique was originally designed [2,3] for tree-level calculations but with superstring [4] and first-quantized [5,6] techniques, it can be extended at least to one-loop diagrams, and with Schwinger representation, it can be extended to multiloops [6,7].

Further simplifications might be obtained by choosing gauges that affect the vertices. The best known example of this kind is probably the background gauge (BG) [8], in which a triple-gluon (3G) vertex attached to an external gluon contains four terms, two less than the six terms present in a normal 3G vertex. This gauge is particularly convenient for one-loop n-gluon one-particle irreducible (1PI) amplitudes, where each 3G vertex present is such a BG 3G vertex. In addition to this reduction in number, of the four terms in such a vertex, only one involves the internal line and needs to be integrated over. For other diagrams a different gauge may be more convenient. For example, in some sense the Gervais-Neveu gauge [9] is the simplest one for n-gluon diagrams in the tree approximation. It is quite remarkable that in tree and one-loop order, the superstring formalism automatically chooses in some sense these best gauges to compute [4].

From these examples it is clear that the most suitable gauge to use depends on the process and the details of the Feynman diagrams. In order to devise new gauges suitable for a new set of Feynman diagrams, a systematic study of the mechanism for the cancellation of gauge-dependent terms is needed. Since Feynman diagrams are much simpler and more intuitive to visualize than the corresponding analytic expressions, it would be best for the same reason if such gauge cancellations can be cast in diagrammatic languages. This is what we intend to develop in the first part of this article.

How this task is accomplished is well known in QED but not in QCD. In QCD, a one-loop *pinching technique* [10,11] is known to simplify calculations by converting ordinary vertices to BG vertices, though to our knowledge a general systematic study for multiloop is not available. There are two reasons why cancellation of gauge-dependent terms and gauge transformations are considerably more complicated in QCD than those in QED. The first is the complication of color. Fortunately, this can be sidestepped by a color decomposition and by the use of color-oriented diagrams, as will be discussed in Sec. II A. The second complication is more substantial, and it relates to the problem of source diffusion. Unlike QED, where the charge always resides on the electron lines, the presence of triple- and four-gluon vertices spreads the color globally throughout the Feynman diagram. In other words, it is the covariant divergence of the color current that is now zero, and not the usual divergence. This global nature means that the local cancellation of gauge dependence in QED is no longer sufficient for QCD. This additional complication of source diffusion fortunately can be handled by introducing "propagating diagrams," as will be discussed in Sec. II B.

One may also view the discussion below in another light. Imagine starting out from a classical Yang-Mills theory or a tree-order scattering amplitude. Ghost vertices are absent there. Suppose now loop diagrams are built up via generalized unitarity by gluing together tree diagrams. Ghost loops would still be absent after the gluing so why then do we need them? The reason must

*Electronic address: feng@physics.mcgill.ca
†Electronic address: lam@physics.mcgill.ca

be that without them the loop amplitudes will no longer be gauge invariant, but how do we see that? Part of what is being discussed below (Figs. 13–16) can be thought of as a way of seeing that. Alternatively, one may think of what is being done below as just another way of deriving the Becchi-Rouet-Stora-Tyutin (BRST) transformation, but this time microscopically, done vertex by vertex and diagram by diagram.

The basic technique for separating the color and for creating the "propagating diagrams" will be discussed in the next section, throughout which the gluon propagator is taken to be in the Feynman gauge. This technique is then used to show *diagrammatically* known field-theoretic results. In particular, covariant gauges will be taken up in Sec. III, and *multiloop* pinching technique will be discussed in Sec. IV, where we shall show how to create background-gauge vertices from ordinary vertices by the *incomplete cancellation* of divergent parts. In Sec. V, we shall discuss two examples how to use these techniques to design new gauges. These are just examples and there is no claim that the new gauges are the simplest possible. Nevertheless, they do illustrate that *simpler* gauges can be designed, and hopefully by working harder, one can some day design the "simplest" gauge to be used for a given set of diagrams. This latter problem is being studied.

II. DIAGRAMMATIC ANALYSIS IN THE FEYNMAN GAUGE

A. Color-oriented vertices

If a QCD Feynman amplitude $\mathcal{T}$ is given a color decomposition into a set of independent color tensors $\mathcal{C}_i$, $\mathcal{T} = \sum_i \mathcal{C}_i a_i$, then each of the color-independent subamplitudes a_i is known to be gauge invariant [1], though how this is achieved diagrammatically, so that individual gauge-dependent diagrams add up to give gauge-independent results, is much less known. In order to study this we must first learn how to compute the subamplitudes a_i diagrammatically.

The relevant diagrams to compute a_i from are the *color-oriented diagrams*. They differ from the ordinary Feynman diagrams in having fixed *cyclic ordering* of the gluon and the ghost lines at all the vertices. Vertices with such ordering imposed are the *color-oriented vertices*; Feynman diagrams made up of color-oriented vertices are the color-oriented diagrams [1,7]. A single Feynman diagram gives rise to many color-oriented diagrams, differing from one another in the cyclic ordering of the gluon and the ghost lines at the vertices. Color-oriented vertices arise from ordinary triple-gluon and ghost vertices by a decomposition of their color factor, $f^{abc} = -i[\mathrm{Tr}(T^aT^bT^c) - \mathrm{Tr}(T^aT^cT^b)]$. The normalization used here is $\mathrm{Tr}(T^aT^b) = \delta^{ab}$. This produces two trace terms with fixed cyclic ordering of the fundamental color generators T^a, corresponding to the two color-oriented vertices. Similarly, the decomposition of the color factor $f^{abcd} = (-i)^2[\mathrm{Tr}(T^aT^bT^cT^d) - \mathrm{Tr}(T^bT^aT^cT^d) - \mathrm{Tr}(T^aT^bT^dT^c) + \mathrm{Tr}(T^bT^aT^dT^c)]$ generates color-oriented vertices for an ordinary four-gluon vertex. The color factor at a fermion vertex is given by T^a. It cannot be further decomposed so there is only one color-oriented vertex per ordinary fermion vertex. In that case it does not matter where the gluon line is drawn with respect to the quark line.

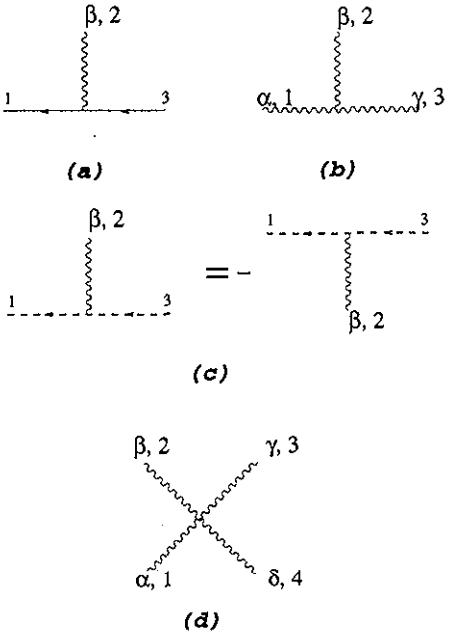

FIG. 1. Color-oriented vertices for QCD.

In a U(N) theory, each color-oriented diagram gives rise to only one color tensor $\mathcal{C}_i$, determined entirely by the cyclic ordering of the external lines. Thus each a_i is given by the sum of color-oriented diagrams with a fixed external-line ordering. For SU(N) theories, a color-oriented diagram may contain more than one color tensor $\mathcal{C}_i$, but in what follows we shall only consider those a_i given by the sum of all color-oriented diagrams with a fixed ordering of the external lines.

With color thus factored out, vertex and propagator factors depend on spin and momentum but no longer on color. The propagators are the usual ones, being $-1/(\gamma\cdot p - m), -1/p^2$, and $g^{\alpha\beta}/p^2$, respectively, for fermions, ghosts, and gluons. Up to a sign the color-oriented vertices coincide with the ordinary vertices without their color factors, which can be read off directly from the coefficients of the interaction Lagrangian density. In this convention, the i's and (2π)'s for the covariant T-matrix element are all collected in a prefactor $[-i/(2\pi)^4]^\ell$, where ℓ is the number of loops. The color-oriented vertices are displayed in Fig. 1; their analytical expressions are given by

$$F_\beta = g\,\gamma_\beta\ , \tag{2.1}$$

$$T_{\alpha\beta\gamma}(p_1,p_2,p_3) = g\,[g_{\alpha\beta}(p_1-p_2)_\gamma + g_{\beta\gamma}(p_2-p_3)_\alpha + g_{\gamma\alpha}(p_3-p_1)_\beta]\ , \tag{2.2}$$

$$G_\beta(p_1) = g\,(p_1)_\beta\ , \tag{2.3}$$

$$Q_{\alpha\beta\gamma\delta} = g^2\,[2g_{\alpha\gamma}g_{\beta\delta} - g_{\alpha\beta}g_{\gamma\delta} - g_{\alpha\delta}g_{\beta\gamma}]\ . \tag{2.4}$$

All momenta in these formulas are outgoing, except those along the quark lines where they follow the directions of the fermionic arrows. The lines in Fig. 1(c) may have two possible orderings, as shown. We shall occasionally refer to the one with a positive sign, as given by Fig. 1(c), to have the *right orientation*, and the one with a minus sign to be of the *wrong orientation*.

B. Divergence relations

A gauge transformation changes the longitudinal polarization of a gluon. The corresponding change to a subamplitude is obtained by computing the divergence of a color-oriented diagram, which in turn is obtained by computing the divergence of the color-oriented vertices. These divergences are obtained from Eqs. (2.1)–(2.4) to be

$$(p_2)^\beta F_\beta = g\ [-(\gamma\cdot p_1 - m) + (\gamma\cdot p_3 - m)]\ , \qquad (2.5)$$

$$\begin{aligned}(p_2)^\beta T_{\alpha\beta\gamma}(p_1,p_2,p_3) = {}& g\ g_{\alpha\gamma}p_1^2 - g\ g_{\alpha\gamma}p_3^2 \\ & -(p_1)_\alpha\ G_\gamma(p_1) \\ & +(p_3)_\gamma\ G_\alpha(p_3)\ , \end{aligned} \qquad (2.6)$$

and

$$(p_2)^\beta G_\beta(p_1) + (p_3)^\gamma G_\gamma(p_1) + g\ p_1^2 = 0\ , \qquad (2.7)$$

$$\begin{aligned}&(p_2)^\beta Q_{\alpha\beta\gamma\delta} - g\ T_{\alpha\gamma\delta}(p_1+p_2,p_3,p_4) \\ &\qquad +g\ T_{\alpha\gamma\delta}(p_1,p_2+p_3,p_4) = 0\ . \end{aligned} \qquad (2.8)$$

The resulting terms have been arranged to be proportional either to a propagator or a vertex so that these relations can be expressed diagrammatically, as in Figs. 2–5. *A cross in a gluon line represents the divergence*, i.e., a factor p_α for the gluon with outgoing momentum p and Lorentz index α. A cross at the end of a (dotted) ghost line is meant to be a cross on the gluon line it is connected to. Namely, if p is the outgoing momentum of the (crossed) ghost line, and α the Lorentz index of the gluon line it is connected to, then a cross at the end of the ghost line indicates a factor $-p_\alpha$. Whenever the propagator of a line is to be included, a dot is put at the end of the line. The propagators in Figs. 2(b), 2(c), 3(b), 3(c), 4(c), 5(b), and 5(c) have been canceled out to obtain these

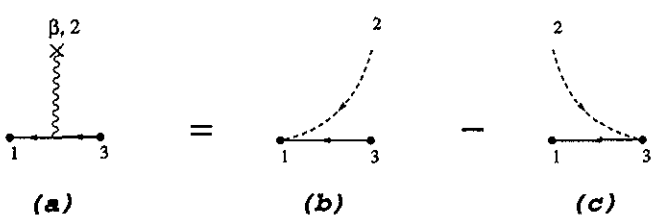

FIG. 2. Divergence relation for the gluon-quark vertex.

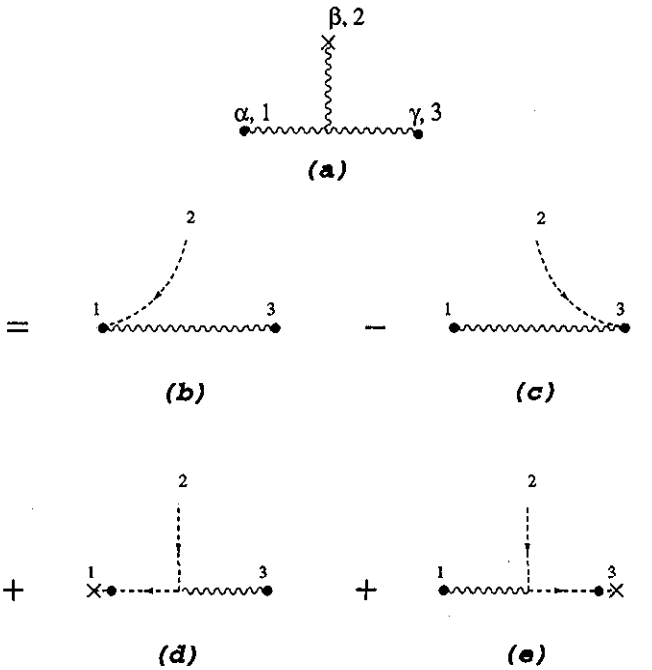

FIG. 3. Divergence relation for the triple gluon vertex.

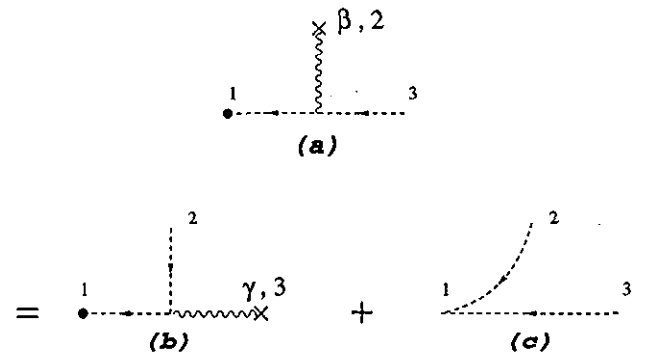

FIG. 4. Divergence relation for the ghost vertex.

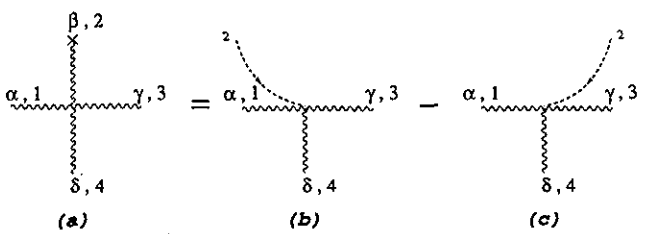

FIG. 5. Divergence relation for the four-gluon vertex.

sliding diagrams, so called because they can be obtained by converting the original gluon line into a sliding ghost (dotted) line. Figures 3(d) and 3(e) serve to propagate the cross along the original gluon lines and will thus be called the *propagating diagrams*. A propagating cross always drags a ghost line behind it, replacing the original gluon line. In order to distinguish this ghost line from the one occurring in ghost loops of Feynman diagrams, we shall occasionally refer to it as the *wandering ghost line*.

QED requires only Fig. 2. What makes QCD complicated is the presence of many more vertices and divergence relations, and the existence of these propagating diagrams relating to the source diffusion problem discussed in the Introduction.

With the possible exception of Fig. 4, these divergence relations have a regular structure which we shall call the *canonical structure*. On the right-hand side of these divergence relations, there are always two sliding diagrams with opposite signs, arranged so that the signs obtained from a triple-gluon vertex are opposite to the signs obtained from a four-gluon vertex. There are no propagating diagrams for the four-gluon vertex, but both of the propagating diagrams emerging from the triple-gluon divergence relation carry a + sign. It turns out that it is this regular canonical structure that guarantees the gauge invariance of the sum of diagrams.

In the sliding diagrams, the wandering ghost line serves to inject a coupling-constant factor g as well as the momentum of the original gluon (p_2) into the line it is tangential to, but otherwise it is inert. Thus if the ghost slides into a momentum-independent vertex, or is tangential to a line whose momentum the vertex does not depend on, then to within a factor of g, the new vertex with the extra ghost line is equal to the old vertex without it, as shown in Figs. 6–8. However, triple-gluon vertices are momentum dependent so Figs. 5(b) and 5(c) are not identical, though their difference is simply given by 5(a).

The signs appearing in Figs. 3(d) and 3(e) require an explanation. First, the crosses in these diagrams are, respectively, $-(p_1)_\alpha$ and $-(p_3)_\gamma$. Second, the original gluon *propagators* for line one in Fig. 3(d), and line three in Fig. 3(e) are now replaced by ghost *propagators*, resulting in an extra minus sign for both. Third, an extra minus sign is attached to the ghost vertex in Fig. 3(d) because of its wrong orientation. Putting these three things together, the signs in front of Figs. 3(d) and 3(e) are both +, a fact which becomes very important later on for ghost cancellation.

Equations (2.5) and (2.6) (Figs. 2, 3) can be used repeatedly to compute the divergence of a color-oriented diagram. This iteration terminates when the cross either rests on (i) an external (wandering) ghost line, or on (ii) a four-gluon vertex like Fig. 5(a), or on (iii) a ghost vertex like Fig. 4(a), or that (iv) there is no longer any cross in the diagram. If (iv) happens, it is possible for the sliding ghost line to end up (iv a) at another external line, (iv b) at a fermion vertex like Fig. 6, (iv c) at a four-gluon vertex like Fig. 7, (iv d) at a ghost vertex like Fig. 8, or (iv e) at a three-gluon vertex like Fig. 5(b) or 5(c).

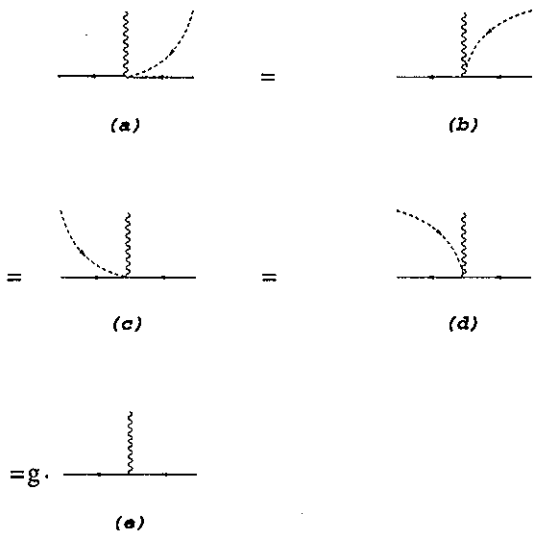

FIG. 6. Relations between sliding diagrams.

C. Notation and conventions

By a "diagram" we always mean a color-oriented diagram from now on. By the "sum of all diagrams" we always mean the sum of all color-oriented diagrams with the same ordering of the external lines as the original diagram.

There are more diagrams in this paper than equations. In order not to confuse diagram numbers with equation numbers, we will adhere to the convention that a number not prefixed by Fig. or Eq. is taken to mean a *diagram number*.

A diagram is said to be *on shell* if all its external lines are on shell. It is said to be *on-shell or crossed* if all its external lines are either on shell, or are off-shell gluon lines carrying a cross. Most of the following results apply either to on-shell diagrams, or on-shell or crossed diagrams.

D. Gauge transformation of color-oriented diagrams

We consider now how a color-oriented diagram changes when the wave function of an external gluon line undergoes a gauge variation. The *change* is proportional to the divergence, represented graphically by a cross at the end of the external gluon line. This produces many diagrams by using 2 and 3, each satisfying one of (i)–(iv) noted above at the end of Sec. II B.

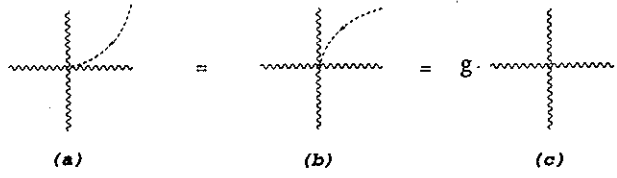

FIG. 7. Diagrams with a ghost line sliding into a four-gluon vertex.

FIG. 8. Ghost vertex with an extra ghost sliding in.

We shall now illustrate how the *net change* from the sum of all diagrams may vanish if the diagrams are taken to be on-shell. This occurs because each resulting diagram either vanishes by itself, or they combine to cancel each other in pairs or in threesome. In the process we will also discover what remains if some of the external lines are taken off shell. These will turn out to be precisely those diagrams required by the BRST transformations.

These conclusions are certainly of no surprise. What we gain by carrying out these analyses is the knowledge how this is realized diagrammatically.

It is simplest to consider first diagrams satisfying condition (iv). When (iv a) is satisfied, the wandering ghost ends on an unamputated external line of the diagram. If this external line is off shell, this diagram survives as is demanded by the BRST transformation. On the other hand, if this is an on-shell line of a scattering diagram, then the propagator must be amputated at the one-particle pole according to the Lehmann-Symanzik-Zimmermann (LSZ) reduction formula. But with a wandering ghost present, the pair of ghost and of external lines no longer possesses a particle pole so these diagrams do not contribute to on-shell (amputated) scattering amplitudes.

Next, suppose (iv b) happens. Then using Fig. 6, a pairwise cancellation takes place as shown in Fig. 9, where diagrams 9(a) and 9(b) to the left of the arrow are the diagrams from which diagrams 9(c) and 9(d) come from one step back in the transformation. Note that Fig. 9, and similarly for all the diagrams considered below, is meant to be a part of a much larger color-oriented diagram, and not necessarily a whole diagram by itself.

Similar pairwise cancellation occurs for (iv c) and (iv d) as shown in Figs. 10 and 11. Using 5, case (iv e) combines

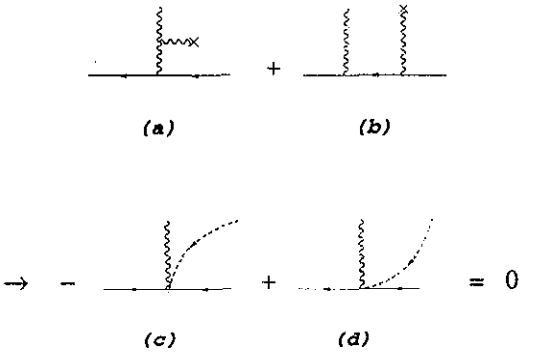

FIG. 9. Local gauge cancellation near a quark vertex.

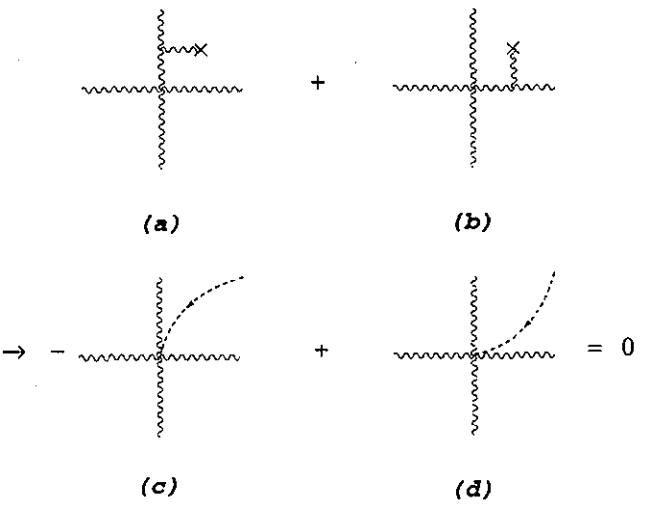

FIG. 10. Local gauge cancellation near a four-gluon vertex.

with case (ii) to give a threesome cancellation as shown in Fig. 12.

Strictly speaking, there is one more case under (iv d) which we have not yet considered, namely, when the wandering ghost line slides into a quadrant bounded by the *outgoing* ghost line, as shown in 15(a) and 15(b). This case will be considered at the end. There are two reasons for the asymmetry between this case and 11, both arising from the asymmetry of the ghost vertex, which depends on the momentum of the outgoing ghost but not on the incoming ghost, nor on the gluon. As a result, the sliding term in 4 slides only to the left but not to the right. Moreover, Fig. 8 is true, but there is no corresponding relation when the wandering sliding ghost lies between the gluon and the *outgoing* ghost.

We must now deal with cases where the wandering ghost line ends at a cross. Case (ii) has already been dealt with but we still have to consider cases (i) and (iii). Case (i) is simple. If that external line the cross eventually ends on is on shell, then an external gluon wave function $\epsilon(p)$ is present, satisfying $p \cdot \epsilon(p) = 0$, so the diagram vanishes. If the gluon line is not on shell, this diagram

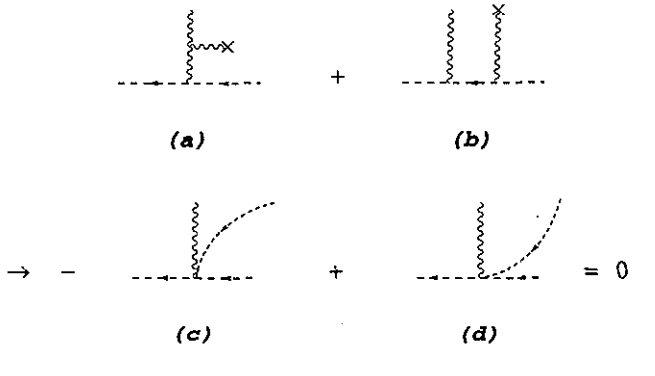

FIG. 11. Local gauge cancellation near a ghost vertex.

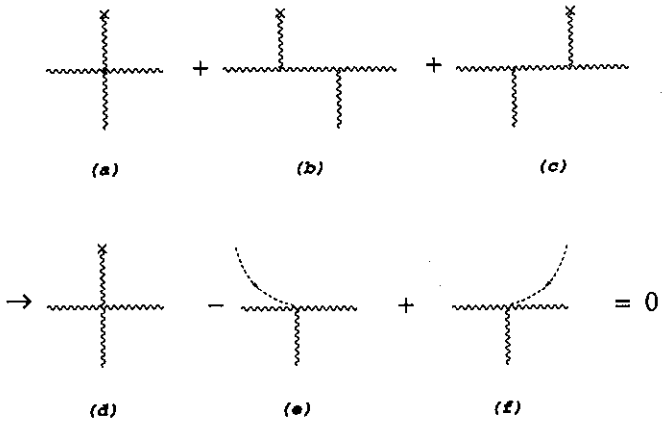

FIG. 12. Local gauge cancellation near a three-gluon vertex.

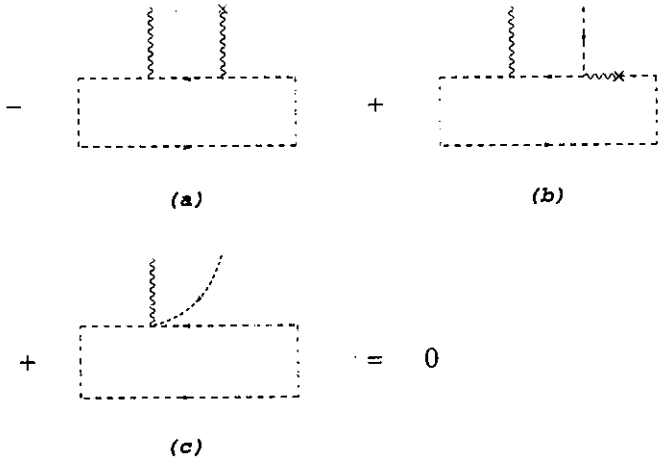

FIG. 13. Cancellation involving ghost loop. Same as Fig. 4 with ghost loop explicitly drawn in.

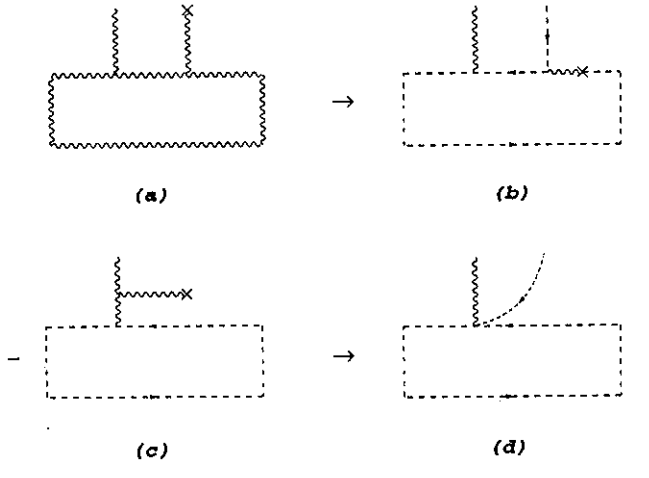

FIG. 14. How 13(b) and 13(c) are produced from color-oriented diagrams.

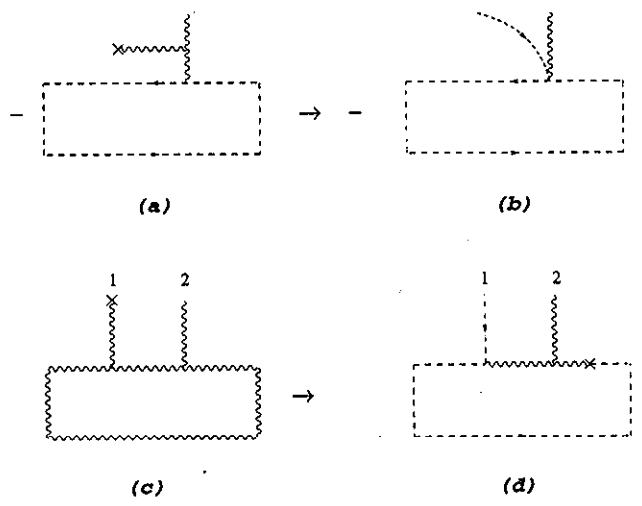

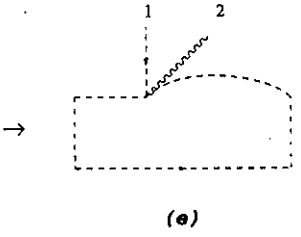

FIG. 15. How 16(a) and 16(b) are produced from color-oriented diagrams.

survives as required by the BRST transformations.

The identity in Fig. 4 is required to deal with case (iii). It is important in this connection to note that the ghost line appearing in 4(a) must be an internal ghost line, forming a closed loop as in 13(a). This means that the identity in 4 will always look like the identity in 13, so the only question left is where 13(b) and 13(c) will come from. With the presence of the ghost loop in 13(a), there must be a diagram where the ghost loop is replaced by a gluon loop, as in 14(a). Using 3(d) and 3(e) repeatedly on 14(a), we shall end up with a diagram that looks like 13(b)=14(b). The minus sign in front of 13(a) comes from the ghost loop factor and there is no corresponding minus sign for the gluon loop in 14(a). In addition to 13(a), there is a diagram like it but the gluon with the cross is linked up directly with the other gluon, as in 14(c). The − sign in front is again because of the ghost

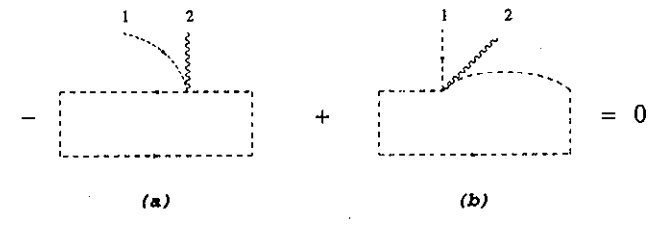

FIG. 16. Pairwise cancellation for the other situation of case (iv d).

loop. Using 3(c) and then the equality in Fig. 8, 14(c) produces 14(d)=13(c). The three diagrams in Fig. 13 cancel one another by using Fig. 4. The same idea will go through if the arrow of the ghost loop in 13(a) runs clockwise instead.

There is one final case which we have not yet dealt with, namely, the other situation of case (iv d) which we skipped before. Consider 15(a), where the explicit $-$ sign in front is again the ghost-loop factor. Using 3(b), this is transferred to 15(b)=16(a), with the wandering ghost between the gluon and the *outgoing* internal ghost line. Its cancellation comes from the gluon-loop diagram shown in 15(c). Using 3(d) and 3(e), 15(c) is transformed into 15(d), which by 3(b), becomes 15(e)=16(b). Now 16(a)+16(b)=0 because the vertices in these two diagrams are simply the same vertex drawn a bit differently.

Note that none of the diagrams in the identities Figs. 2–16 ever appear twice, so double counting can never occur. Moreover, each conceivable configuration appears in one of these identities, so by using all possible identities, there can never be an uncanceled term. For that reason the sum of all on-shell diagrams with a cross at the end of a gluon line must be zero.

The "proof" above is not mathematically rigorous in that we have not explicitly enumerated all the possible topologies and structures of diagrams. Nevertheless, it fulfils our main aim in demonstrating how gauge cancellation between diagrams occurs in each specific instance.

III. COVARIANT GAUGES

The gluon propagator in a covariant gauge is $(g^{\alpha\beta} + \xi p^\alpha p^\beta/p^2)/p^2$. In the last section, divergence relations and gauge invariances of the external gluons were shown in the Feynman gauge $\xi = 0$. The effect of $\xi \neq 0$ will be discussed in the present section, using the same techniques developed in the last.

The only additional tool needed for the following analysis is the double-divergence relation

$$(p_3)^\gamma (p_2)^\beta T_{\alpha\beta\gamma}(p_1,p_2,p_3) = g\,(p_3)_\alpha p_1^2 - (p_1)_\alpha (p_3)^\gamma G_\gamma(p_1)\ , \quad (3.1)$$

obtainable from Eq. (2.6) by taking the divergence with respect to p_3 on both sides. Diagrammatically, this can be represented by Fig. 17, which is the same as Fig. 3 with 3(b) and 3(e) removed and with an additional cross added to the third gluon line. A convenient way to remember this is to regard Fig. 3 to be true at all times, with or without an additional cross on line 3, with an additional stipulation that the ghost line on the right-hand side must avoid coming into contact with any additional cross. This stipulation effectively eliminates 3(b) and 3(e) as required.

This double-divergence relation allows us to generalize the result of the Sec. II D into the following rule.

R1. *The sum of all on-shell or crossed diagrams with a cross on one of the external gluon lines is zero, if all gluon propagators are taken in the Feynman gauge.*

This result is more general than what has been discussed because the external lines with a cross on them do not have to be on shell, so diagrams of types (iv a) and (i) with the wandering ghost resting on them will no longer vanish. However, such diagrams can never occur because of Eq. (3.1), which, as noted before, may be taken to say that the wandering ghost line must avoid the additional crosses now situated at the end of the off-shell gluon lines.

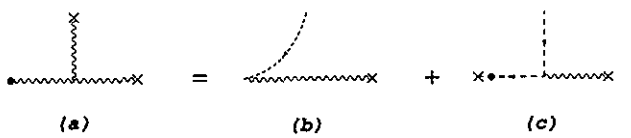

FIG. 17. Double-divergence relation of the triple gluon vertex.

This result can be used to show the independence of the gauge parameter ξ.

R2. *The sum of on-shell or crossed diagrams is independent of the gauge choice of every gluon propagator.*

The gauge-dependent part of a gluon propagator is of the form $\xi p^\alpha p^\beta/p^2/p^2$. Except for the additional factor $\xi/p^2/p^2$, the ξ-dependent part can be represented diagrammatically by breaking the internal line into a pair of external lines, each with a cross at the end. In this way, two diagrams are generated by each gluon propagator: one being the original diagram with the propagator in the Feynman gauge, and the other obtained by breaking this propagator into a pair of external lines with a cross at the end of each.

If a diagram has m propagators, then this procedure breaks it up into 2^m diagrams. When we sum up all possible on-shell–crossed diagrams, the sum becomes 2^m sets of sums, each of which satisfies **R1**, thus establishing **R2**.

IV. PINCHING TECHNIQUE AND THE BACKGROUND GAUGE

The technique developed in Sec. II can also be used to manipulate the divergence part of a triple-gluon vertex. Such vertex manipulations had previously been used to simplify one-loop calculations, and in that context it is known as the *pinching technique* [10]. To one-loop order it has been shown that pinching technique gives rise to the *background gauge* (BG) [11]. In what follows, we generalize this approach to *multiloops* to show how to convert the normal vertices into the BG vertices.

A. BG vertices

The BG color-oriented vertices consist of the original vertices in Fig. 1 [Eqs. (2.1)–(2.4)], plus the additional vertices in Fig. 18 given by the formulas

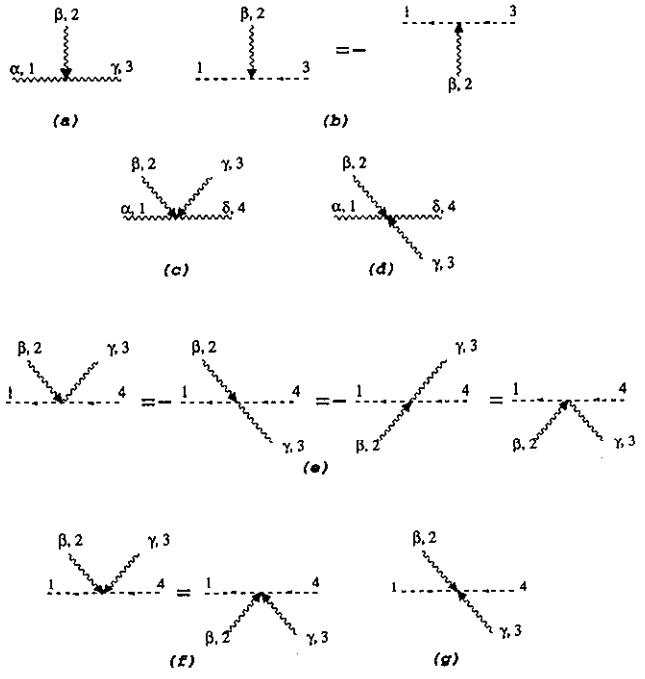

FIG. 18. Color-oriented BG vertices with at least one arrowed (external) line.

$$[18(a)] = g\,[g_{\gamma\alpha}(p_3 - p_1)_\beta - 2g_{\alpha\beta}(p_2)_\gamma + 2g_{\beta\gamma}(p_2)_\alpha]\,, \tag{4.1}$$

$$[18(b)] = g\,(p_1 - p_3)_\beta\,, \tag{4.2}$$

$$[18(c)] = g^2\,[-g_{\beta\gamma}g_{\alpha\delta} - 2g_{\alpha\beta}g_{\gamma\delta} + 2g_{\alpha\gamma}g_{\beta\delta}], \tag{4.3}$$

$$[18(d)] = -2g^2\,g_{\beta\gamma}g_{\alpha\delta}\,, \tag{4.4}$$

$$[18(e)] = g^2\,g_{\beta\gamma}\,, \tag{4.5}$$

$$[18(f)] = g^2\,g_{\beta\gamma}\,, \tag{4.6}$$

$$[18(g)] = -2g^2\,g_{\beta\gamma}\,. \tag{4.7}$$

Gluon lines with an arrow are to be distinguished from gluon lines without an arrow. In this section we follow the traditional usage to assume all arrowed lines to be external gluon lines, though the reverse is not true. The correct vertices to use in BG are obtained through explicit calculations. The results of these calculations are summarized diagrammatically in Figs. 18 and 1, provided we adopt the following convention. Vertices attached to external gluon lines should be taken from 18 whenever possible, but if they are absent from 18, then they should be taken from 1. For example, triple-gluon vertices with two external gluons and quark-gluon vertices with an external gluon are not to be found in 18, so they should be taken from 1(b) and 1(a), respectively.

It is this distinction between external and internal gluons that produces so many vertices in the BG. In spite of this complication, it is often still simpler to calculate loop processes with a large number of external gluon lines in the BG, because of its reduced dependence on the internal momenta of a triple-gluon vertex. BG is also the gauge that emerges naturally in superstring calculations for 1PI diagrams [4].

The equivalence between the ordinary and the BG vertices can be stated as follows.

B. R3

The sum of on-shell or crossed diagrams are not affected when the vertices attached to any number (n) of external gluon lines are changed from the ordinary vertices (Fig. 1) to the BG vertices (Figs. 1 and 18).

C. Creation of the new BG vertices

To demonstrate **R3** we need to know how the new BG vertices in Fig. 18 are related to the ordinary vertices in Fig. 1. These relations can be obtained from a relation between 1(b) and 18(a), or equivalently between Eqs. (2.2) and (4.1), shown graphically in Fig. 19. For this purpose, it is necessary to introduce a new vertex with two gluon lines and one ghost line [19(b) and 19(c)], joined together by a circle representing the factor $\pm g\,g_{\mu\nu}$, where μ, ν are the Lorentz indices of the two gluon lines. The sign is taken to be + for 19(c) and − for 19(b). This sign convention is chosen to be the same as the ordinary ghost vertex 1(c) if the incoming ghost line is replaced by the arrowed gluon line. In the terminology introduced below Eq. (2.4), 19(c) has the right orientation and 19(b) has the wrong orientation. From now on we shall refer to the vertices 19(b) and 19(c) as the *funny vertices.*

Figure 19 is used to convert an ordinary vertex 19(a) to a BG vertex 19(d). The two extra terms 19(b) and 19(c) will be shown to be instrumental in converting other ordinary vertices into BG vertices. This proceeds by induction on n, the number of external lines at which such conversion of vertices is desired.

Suppose $n = 1$ and an ordinary vertex 19(a) attached with a single external gluon line is converted into the BG vertex 19(d). The effect of the extra term 19(b) will now

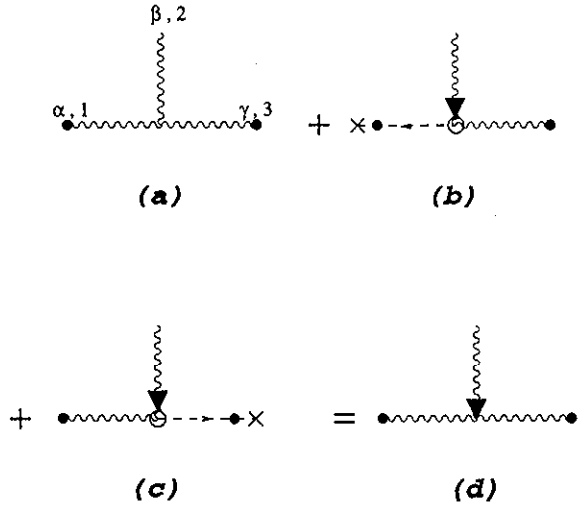

FIG. 19. Relation between the triple-gluon vertices 1(b) and 18(a).

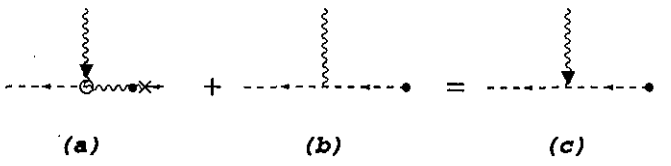

FIG. 20. Generation of the ghost vertex 18(b).

be explained, and an analogous result exists for 19(c). If we remove the bulk of the vertex 19(b) from a diagram except for its cross, **R1** is applicable to the remaining diagram, so the extra diagrams generated by 19(b) will add up to zero, except when the crosses in 19(b) are returned by propagation to the same vertex via a gluon loop. In that case 19(b) gives rise to 20(a), in which the gluon loop linking the two sides of the funny vertex is now converted to a ghost loop trailing the cross. There exists another diagram where the gluon loop is replaced by the ghost loop, in which the ordinary ghost vertex 20(b) appears. The combination of 20(a) and 20(b) now gives rise to the BG ghost vertex 20(c). An extra minus sign from the ghost loop has been incorporated in front of 20(a) to make the combined sign + as shown. However, analytically 20(a) contributes a minus sign because of the wrong orientation of the funny vertex.

The only other way the cross in 19(b) can return is through a sliding diagram 3(b) at the last step, thus producing 21(a) or 22(a). Since the propagating cross always drags a ghost line behind it, the gluon loop through which the cross returns has now been changed into a ghost loop and an examination of Eqs. (4.5) and (4.6) shows that 21(a) is the same as 21(b)=18(e) and 22(a) is the same as 22(b)=18(e) and 22(c)=18(f).

We have therefore completed showing **R3** when $n = 1$, because none of the other BG vertices in 18 are present for $n = 1$.

We will now proceed to $n = 2$ and assume the first vertex to have already been converted into BG vertex. We must now examine the effect of converting the second vertex from ordinary to BG vertex, again using the relations in 19. Clearly as in the case $n = 1$, there is no problem in converting the second vertex into BG vertex if it was alone. But with $n = 2$, there is now the possibility of an interaction between the two vertices to cause a change.

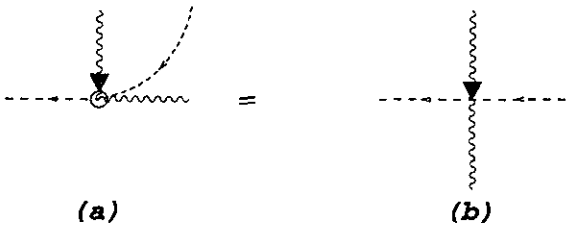

FIG. 21. Generating the ghost vertex 18(e).

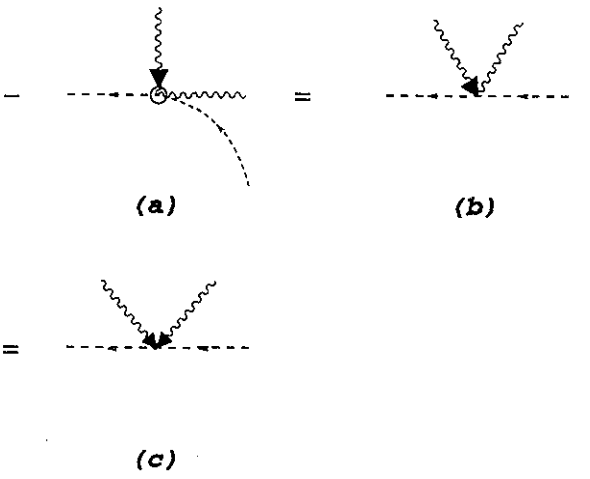

FIG. 22. Generating the ghost vertices 18(e) and 18(f).

To start with, we can no longer use Fig. 3 to propagate the cross beyond the first vertex because the triple-gluon vertex here is already a BG vertex. We must therefore work out a relation analogous to 3 but valid for the BG triple-gluon vertex. This is obtained from Eq. (4.1) and shown in 23, with 23(f) being $-g\, g_{\alpha\gamma}(p_2)^2$. It is important to note that this divergence still possesses a regular structure. As before, we have the sliding diagrams with opposite signs [23(b) and 23(c)], the propagating diagrams with plus signs [23(d) and 23(e)], but there is now a new *stagnant diagram* involving the funny vertex [23(f)] with a single ghost line that goes nowhere. The analytical expression for this term is $-p_2^2 g_{\alpha\gamma}$, with a minus sign on account of the wrong orientation of the funny vertex. Note also that the gluon line in 23(d) has an arrow but not the one in 23(e), "because" that is how it is inherited from 23(a).

Although this is getting ahead of ourselves, it would be

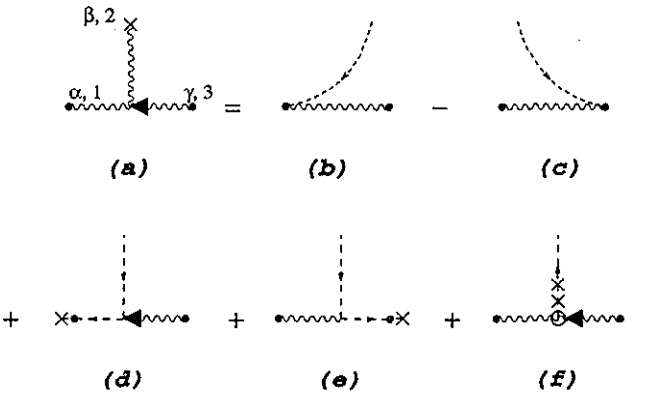

FIG. 23. Divergence relation of the BG triple-gluon vertex 18(a).

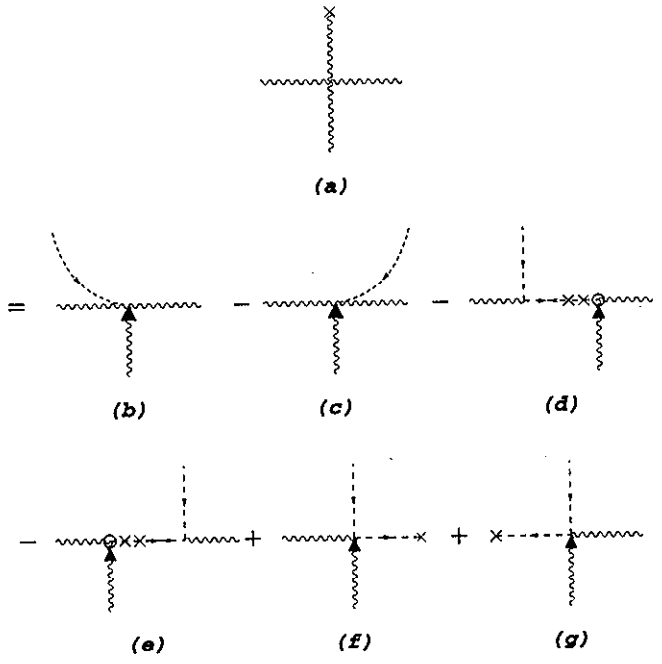

FIG. 24. Divergence relation of the four-gluon vertex 1(d) expressed in terms of BG vertex. The cross is opposite to the external line in the four-gluon vertex.

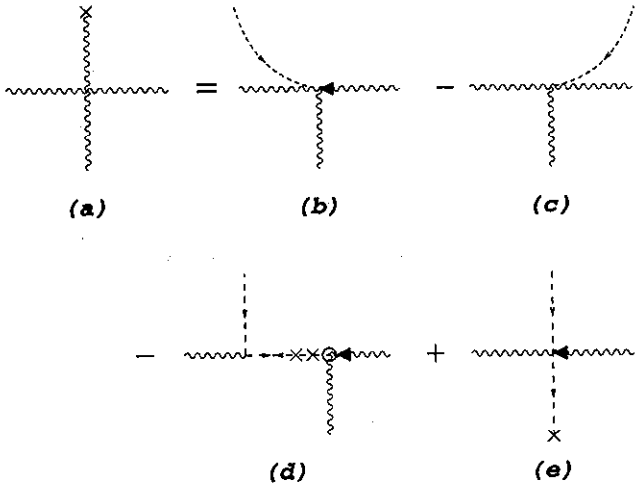

FIG. 26. Divergence relation of the four-gluon vertex 1(d) expressed in terms of BG vertex. The cross is adjacent to the external line in the four-gluon vertex.

useful for the sake of comparison to examine this *modified canonical structure* for other divergence relations obtained from Eqs. (4.1)–(4.7), and shown in Figs. 24–29. There are unfortunately many divergence relations, but this cannot be helped because there are many BG vertices, and because there are many external-line–cross combinations in taking the divergence of 1(d). Nevertheless, all these relations possess the sliding diagrams with the canonical signs, the propagating diagrams with plus signs, and the stagnant diagrams with minus signs. External lines are inherited, vertices that do not make sense will not appear, and in the case of the divergence of a four-gluon vertex, the cross is not allowed to propagate through an arrowed line. This last rule is "why" there are no propagating ghosts from the top to the bottom gluon lines in 24, for example. The reason "why" there is no propagating ghost from the top to the left line in Fig. 26 is because the resulting BG ghost vertex does not exist (the arrowed line is not adjacent to the outgoing ghost).

The signs contained in this modified canonical structure are precisely correct to make the extraneous diagrams cancel, extraneous meaning those not needed to

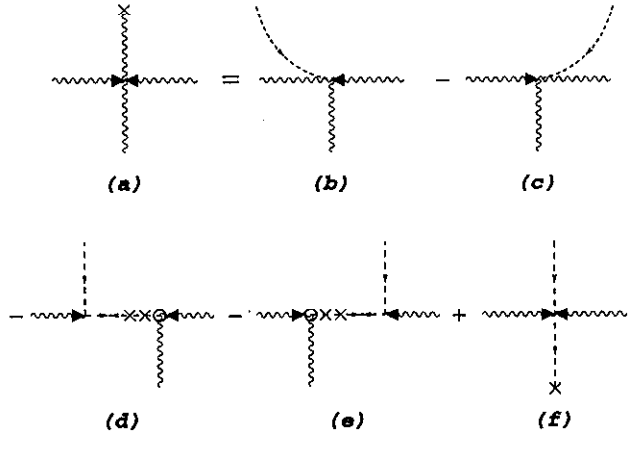

FIG. 25. Divergence relation of the four-gluon vertex 18(d) expressed in terms of the BG vertex.

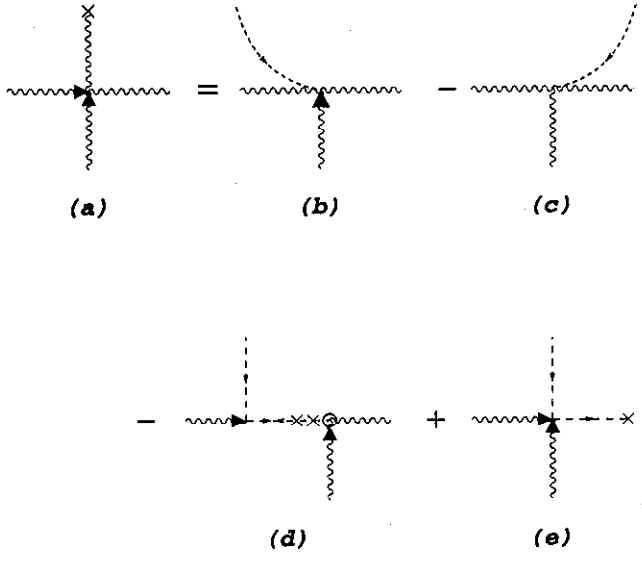

FIG. 27. Divergence relation of the four-gluon vertex 18(c) expressed in terms of the BG vertex.

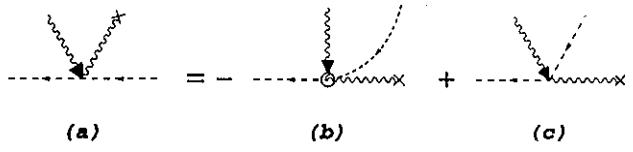

FIG. 28. Divergence relation of the ghost vertex 18(e) expressed in terms of the BG vertex. The cross is adjacent to the arrowed line.

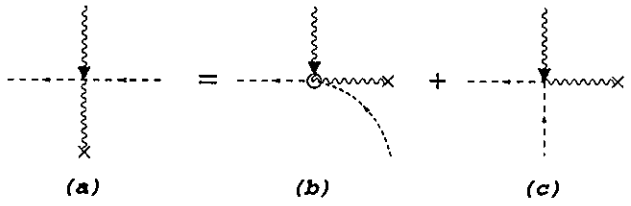

FIG. 29. Divergence relation of the ghost vertex 18(e) expressed in terms of the BG vertex. The cross is opposite to the arrowed line.

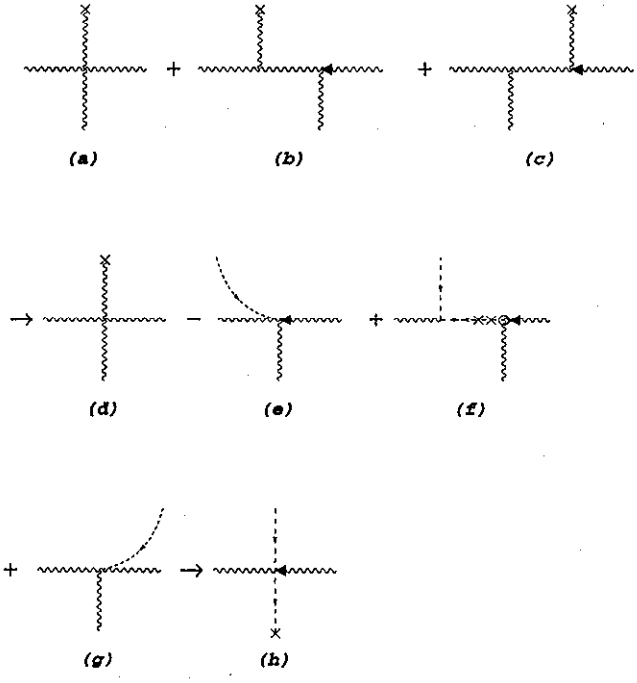

FIG. 30. An example of local gauge cancellations, leaving behind just a propagating term to work on another vertex.

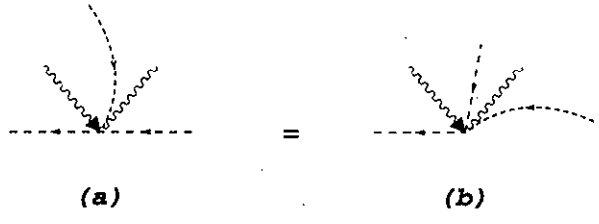

FIG. 31. Equality of a ghost line sliding into the ghost vertices 18(e).

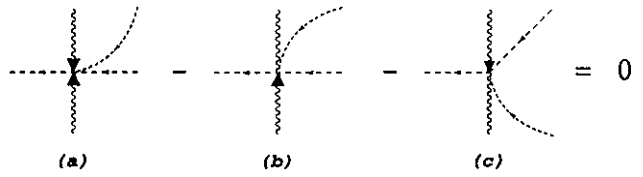

FIG. 32. Equality of a ghost line sliding into the ghost vertices.

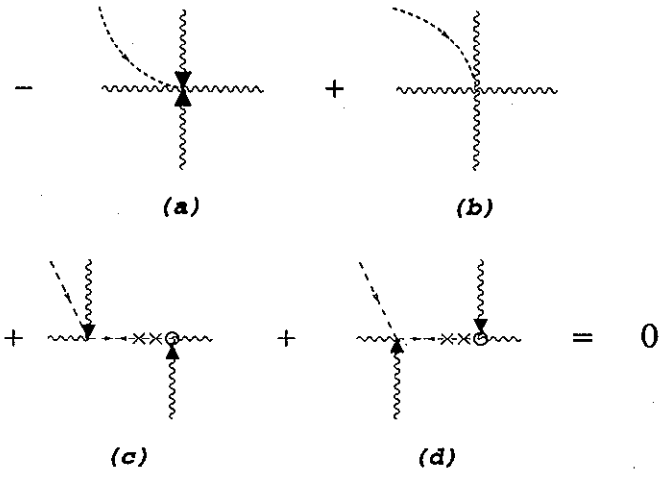

FIG. 33. Equality of a ghost line sliding into four-gluon vertices.

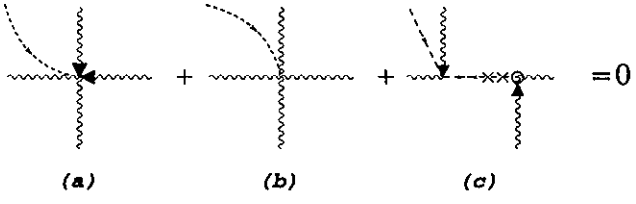

FIG. 34. Equality of a ghost line sliding into four-gluon vertices.

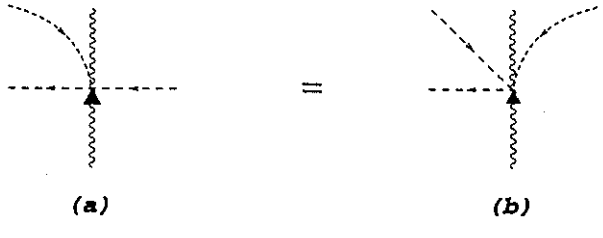

FIG. 35. Equality of a ghost line sliding into the ghost vertices 18(e).

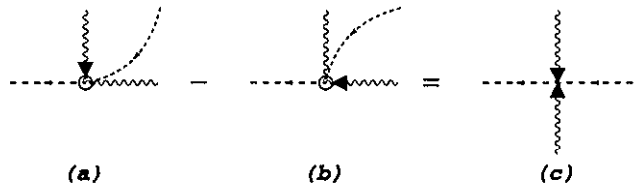

FIG. 36. Generating the ghost vertex 18(g).

produce new BG vertices. For example, consider the combination of diagrams 30(a), 30(b), and 30(c). By using 3 and then 23, 30(b) produces 30(e) and 30(f), and 30(c) produces 30(g). Using 26, these combine to cancel, leaving behind only the propagating diagram 30(h) to move on to other vertices.

Similar cancellation takes place in all other cases, if we take into account other identities shown in 31–35.

It is important to remark that in the definition of the BG vertices 18–22 and 36–38, as well as in the divergence relations 23–29, all the external lines may be taken off shell.

Let us now return to the construction of the BG vertices for $n = 2$, and consider the effect of the cross 19(b) originating from the second vertex reaching the first (BG) vertex. Because of the modified canonical structure of 26, things proceed similarly to **R1** and **R2**. Various situations can happen when this cross returns to vertex 2 via a gluon loop. A sliding contribution just before it returns to the second vertex gives rise to 21, 22, and 36.

If the first vertex is just to the right of the second vertex, then in using 19 to convert the second vertex, the contribution of 19(c) followed by 23 on the first vertex produces terms like 37(b), 38(b), and 38(c). When combined with ordinary four-gluon vertex attached to these two external lines, the BG vertices 37(c) and 38(d) are produced.

This completes the demonstration of **R3** for $n = 2$. For $n > 2$, it is easy to see that nothing new can happen, in the sense that three or more vertices can interact only pairwise, so the result is expected to be true for all n.

V. EXAMPLES OF NEW GAUGES

The technique developed in Sec. II was used in Sec. III to show the independence of the gauge used in gluon propagators, and in Sec. IV to convert ordinary vertices to BG vertices. There is no reason why it cannot be used

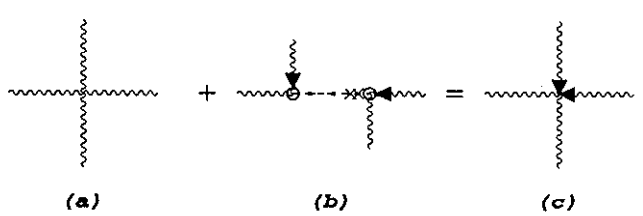

FIG. 37. Generating the four-gluon vertex 18(c).

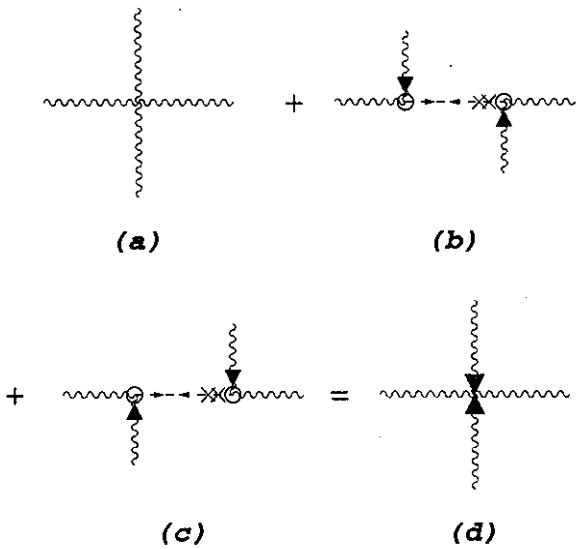

FIG. 38. Generating the four-gluon vertex 18(d).

to study other gauge problems, including our eventual hope to find the "best" gauge for computing a specific set of gauge-invariant diagrams.

In the present section, we will discuss two unconventional gauges, one for four-gluon tree amplitude and the other for two-loop gluon self-energy diagrams. The new gauges carry fewer terms than either the ordinary or the BG gauge. Though they may not be the "best" gauge possible for the specific problems, nevertheless, they do illustrate the fact that improvements can be made on existing gauges using the techniques developed in this paper.

The tree-diagram example is given in Fig. 39, where the arrowed vertices are given in 18 [Eqs. (4.1) and (4.4)]. It can be shown using the techniques above that a new gauge containing the vertices in these diagrams does exist, viz., the three diagrams in 39 do sum up to give the four-gluon on-shell scattering amplitude.

Note that this is *not* the BG gauge. Since all the four lines in 39(a) are external, vertex 1(d) should be used in the background gauge instead of 39(a). Moreover, each of the two 3G vertices in 39(b) and 39(c) contains two external lines, again 1(b) rather than 18(a) should have been used in the background gauge. In other words, there is no difference between the BG and the ordinary gauge in this process.

Figure 39(a) contains one term but the corresponding vertex in BG contains three terms. Each of 39(b) and

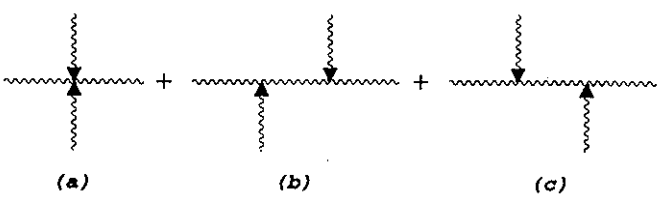

FIG. 39. Four-gluon tree amplitude in a new gauge.

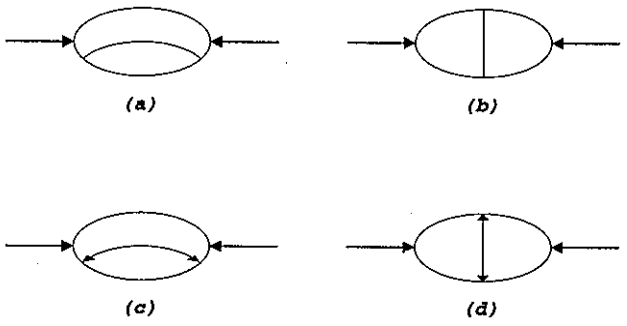

FIG. 40. Diagrams with two gluon loops for the gluon self-energy in the BG gauge [(a) and (b)] and in the new gauge [(c) and (d)].

39(c) contains $4^2 = 16$ terms whereas the corresponding diagrams in BG each contains $6^2 = 36$ terms. Thus the new gauge depicted in 39 saves a total of 42 terms out of the 75 terms needed in the BG.

The two-loop example is given in Fig. 40, where for easy drawing, solid lines are used to denote gluons. Figures 40(a) and 40(b) are the two-gluon-loop diagrams in BG, whereas 40(c) and 40(d) are the same diagrams in the new gauge. Again the arrowed vertices are those displayed in 18. The two-loop gluon self-energy contains a total of 18 diagrams in BG, but owing to incomplete cancellation of the divergence terms when we shift gauges, new vertices and new diagrams are generated and a total of 23 diagrams appeared in this new gauge [12]. Nevertheless, the new gauge still contains few terms in total, because the largest number of terms for each gauge already occurs in the diagrams shown. The BG contains a total of 1367 terms, of which 1152 are contained in 40(a) and 40(b). In contrast, the new gauge contains a total of only 860 terms, of which 512 are contained in 40(c) and 40(d). In other words, 62% more labor is required to compute the two-loop self energy in BG than in the new gauge, and clearly even more labor is required to compute it in the ordinary gauge.

Other details of this gauge and the two-loop computation will appear separately.

ACKNOWLEDGMENTS

This research was supported in part by the Natural Science and Engineering Research Council of Canada and by the Québec Department of Education. Y.J.F. acknowledges the support of the Carl Reinhardt Major Foundation. C.S.L. thanks F. Wilczek for discussions and hospitality at the Institute for Advanced Study, Princeton where part of this manuscript was written.

[1] R. Gastmans and Tai Tsun Wu, *The Ubiquitous Photon Helicity Method for QED and QCD* (Clarendon Press, London, 1990); M.L. Mangano and S.J. Parke, Phys. Rep. **200**, 301 (1991).

[2] F.A. Berends, R. Kleiss, P. De Causmaecker, R. Gastmans, W. Troost, and T.T. Wu, Phys. Lett. **103B**, 124 (1981); Nucl. Phys. **B206**, 61 (1982); **B239**, 382, 395 (1984); **B264**, 243, 265 (1986).

[3] Z. Xu, D.-H. Zhang, and L. Chang, Tsinghua University, Beijing, China, Report No. TUTP-84/4 (unpublished); Report No. TUTP-84/5 (unpublished); Report No. TUTP-84/6 (unpublished); Nucl. Phys. **B291**, 392 (1987).

[4] Z. Bern and D.C. Dunbar, Nucl. Phys. **B379**, 562 (1992); Z. Bern and D.A. Kosower, Phys. Rev. Lett **66**, 1669 (1991); Nucl. Phys. **B362**, 389 (1991); **B379**, 451 (1992); Z. Bern, L. Dixon, and D.A. Kosower, Phys. Rev. Lett. **70**, 2677 (1993).

[5] M. Strassler, Nucl. Phys. **B385**, 145 (1992); SLAC Report No. SLAC-PUB 5978, 1992 (unpublished).

[6] M.G. Schmidt and C. Schubert, Phys. Lett. B **331**, 69 (1994).

[7] C.S. Lam, Nucl. Phys. **B397**, 143 (1993); Phys. Rev. D **48**, 873 (1993); Can. J. Phys. **72**, 415 (1994); Y.J. Feng and C.S. Lam, Phys. Rev. D **50**, 7430 (1994).

[8] B.S. DeWitt, Phys. Rev. **162**, 1195, 1239 (1967); in *Dynamic theory of groups and fields* (Gordon and Breach, New York, 1965); G. 't Hooft, Nucl. Phys. **B62**, 444 (1973); L.F. Abbott, *ibid.* **B185**, 189 (1981).

[9] J.L. Gervais and A. Neveu, Nucl. Phys. **B46**, 381 (1972).

[10] J.M. Cornwall, in *Proceeding of the French-American Seminar on Theoretical Aspects of Quantum Chromodynamics*, Marseille, France, 1981, edited by J.W. Dash (Centre de Physique Théorique, Marseille, 1982); Phys. Rev. D **26**, 1453 (1982); J.M. Cornwall and J. Papavassiliou, *ibid.* **40**, 3474 (1989); J. Papavassiliou, *ibid.* **41**, 3179 (1990); Phys. Rev. D **47**, 4728 (1993); G. Degrassi and A. Sirlin, *ibid.* **46**, 3104 (1992).

[11] A. Denner, G. Weiglein, and S. Dittmaiser, Phys. Lett. B **333**, 420 (1994); S. Hashimoto, J. Kodaira, Y. Yasui, and K. Sasaki, Phys. Rev. D **50**, 7066 (1994).

[12] Y.J. Feng and C.S. Lam (unpublished).